Reproductive Sciences (2023) 30:247–257
https://doi.org/10.1007/s43032-022-01004-y

MALE REPRODUCTION: ORIGINAL ARTICLE

Reduction of SLC7A11 and GPX4 Contributing to Ferroptosis in Sperm from Asthenozoospermia Individuals

Xiaoling Hao[1,2] · Hong Wang[2,3] · Fang Cui[4] · Zihan Yang[1,2,5] · Liu Ye[1] · Run Huang[1] · Jiangping Meng[1]

Received: 27 December 2021 / Accepted: 7 June 2022 / Published online: 21 June 2022

Abstract

Ferroptosis is a newly defined form of regulated cell death, which is involved in various pathophysiological conditions. However, the role of ferroptosis in male infertility remains unclear. In this study, 42 asthenozoospermic and 45 normozoospermic individuals participated. To investigate the ferroptosis level in the two groups, the levels of reactive oxygen species (ROS), malondialdehyde (MDA), and iron were measured, and mitochondrial membrane potential (MMP) was detected as an indicator of mitochondrial injuries. Compared with the normozoospermic group, ROS ($p < 0.05$), MDA ($p < 0.001$), and iron ($p < 0.001$) of the asthenozoospermic group were significantly increased. However, the asthenozoospermia group had a decreased MMP level ($p < 0.05$). In addition, the expression levels of GSH-dependent peroxidase 4 (GPX4) ($p < 0.001$) and solute carrier family 7 member 11 (SLC7A11) ($p < 0.05$) were also reduced in asthenozoospermic individuals. In asthenozoospermic samples, a significantly high positive correlation was observed between GPX4 mRNA levels and progressive motility ($r = 0.397$, $p = 0.009$) and total motility ($r = 0.389$, $p = 0.011$), while a negative correlation was observed between GPX4 and iron concentration ($r = -0.276$, $p = 0.077$). The function of ferroptosis in asthenozoospermic males has never been studied before. In our study, we concluded that GPX4 and SLC7A11 expression levels in asthenozoospermia patients were related to increased ferroptosis and impaired sperm function, revealing novel molecular insights into the complex systems involved in male infertility.

Keywords Ferroptosis · ROS · Asthenozoospermia · Semen quality · Male infertility

Introduction

Infertility is a social and medical problem that affects 15% of couples worldwide [1]. According to a previous report, the male factor accounts for up to 50% of all infertile couples [2]. Asthenozoospermia is a major cause of infertility and is represented as reduced or absent sperm motility in the semen sample, which is defined as the semen sample containing less than 40% sperm motility and less than 32% sperm progressive motility [3]. Many theories have been proposed to reveal the mechanism of asthenozoospermia, including mitochondrial disfunction, genetic defects, and hormonal disturbances [4–6]. However, the etiology of asthenozoospermia is not completely understood.

Reactive oxygen species (ROS) are a cause of male infertility. ROS refer to a group of highly reactive chemicals formed from oxygen, including superoxide, hydroxyl radicals, and singlet oxygen [7]. According to previous reports, a physiological level of ROS is believed to be

Xiaoling Hao and Hong Wang contributed equally to this work and should be regarded as co-first authors.

✉ Jiangping Meng
mjlily2000@163.com

1 Reproductive Medicine Center, Department of Obstetrics and Gynecology, The First Affiliated Hospital of Chongqing Medical University, Chongqing, China

2 Key Laboratory of Diagnostic Medicine Designated By the Ministry of Education, Chongqing Medical University, Chongqing, China

3 School of Laboratory Medicine, Chongqing Medical University, Chongqing, China

4 Department of Laboratory Medicine, The First Affiliated Hospital of Chongqing Medical University, Chongqing, China

5 Sichuan Provincial Maternity and Child Health Care Hospital, No. 290, Shayan West Second Street, Wuhou District, Chengdu City, Sichuan Province, China

required for sperm motility, hyperactivation, and capacitation, as well as acrosome reaction [8, 9]. Nevertheless, many recent studies on oxidative stress have shown that ROS play a significant role in the pathological mechanism of male infertility. Excessive ROS can impair sperm motility not only through lipid peroxidation but also by interfering with antioxidant enzymes and oxidation proteins in sperm [10, 11]. The semen of asthenoteratozoospermic men also produces more ROS than that of normal men [12].

Ferroptosis is a reactive oxygen species (ROS)-dependent cell death derived from free iron overload (FIO), ROS production, and lipid peroxidation. In humans, the pervasive impact of ferroptosis has been linked to the development of various diseases such as Alzheimer's disease, cancer, and heart disorders [13–15]. However, the role of ferroptosis in male infertility has not been fully elucidated. Ferroptosis inhibition is a promising approach to treating arsenite-induced testicular toxicity in relevant research [16]. Ferroptosis was detected at a high level in human sperm from heavy smokers and was thought to affect sperm quality [17]. Furthermore, a study implied that busulfan-induced oligospermia can be attenuated by inhibition of ferroptosis in mice [18]. Hence, we reasoned that ferroptosis may impair sperm quality in asthenozoospermia.

GSH-dependent peroxidase 4 (GPX4), a crucial antioxidant enzyme in mammals that protects cells from lipid peroxidation, can be hindered directly to initiate ferroptosis [19, 20]. Intriguingly, GPX4 is abundantly expressed in reproductive organs and spermatozoa, and one study found that 10% of infertile men had dramatically decreased sperm GPX4 expression, indicating that GPX4 is vital for male fertility [21]. Solute carrier family 7 member 11 (SLC7A11), a crucial component of the cystine/glutamate transporter system Xc^-, promotes the absorption of cystine and the production of GSH, which protects cells against oxidative stress and ferroptosis [22, 23]. GSH is the reducing substrate of GPX4 activity. According to research, lowering the levels of SLC7A11 leads to a reduction in intracellular cystine levels and, as a result, a reduction in GSH production, which, in turn, suppresses GPX4 activity and, as a result, activates ferroptosis [24, 25]. However, the biological mechanism underlying the depletion or downregulation of GPX4 and SLC7A11 in asthenozoospermia remains unclear.

In this study, semen samples from asthenozoospermic patients and normozoospermic men were obtained, and we aimed to determine whether ferroptosis can impact the status of sperm motility and be involved in the occurrence of asthenozoospermia. Our findings provide a novel mechanism underlying the etiology of asthenozoospermia and propose a possible route to treat male infertility.

Materials and Methods

Sample Collection

Forty-five normozoospermic donors and 42 asthenozoospermic men were enrolled. The semen characteristics of asthenozoospermic men were considered sperm concentrations $\geq 15\times10^{\wedge6}$ cells per mL, progress motility $< 32\%$ or total sperm motility $\leq 40\%$ at 1 h after ejaculation, and normal sperm morphology $\geq 4\%$. In addition, the following exclusion criteria were defined: leucocyte and round cell concentration $> 10^{\wedge6}$/mL of ejaculate, history of smoking, alcohol and drug abuse, hypertension, and varicocele. Routine sperm parameter analysis, including motility, morphology, and count, was performed according to the World Health Organization (WHO) standards. Analysis of sperm motility was performed using computer-aided sperm analysis (CASA) software (Beion, China).

Semen Preparation

All samples were collected by masturbation following 3–5 days of sexual abstinence and allowed to liquefy at room temperature. Semen was taken from sterilized containers and centrifuged at 80% and 40% Percoll gradient centrifugation to isolate highly motile sperm. Different types of cells remained in the top segment of the tube and were removed by pipetting. The remaining sperm pellet was washed with PBS twice at $800\times g$ for 5 min and resuspended in BWW medium (Solarbio, China) for subsequent experiments.

Measurement of the Production of Reactive Oxygen Species

The amount of ROS in the spermatozoa was detected using an oxidation-sensitive fluorescent probe called 2′,7′-dichlorofluorescein diacetate (DCFH-DA; Beyotime, China). In brief, 20×10^6 spermatozoa were suspended in 1000 µL of DCFH-DA (10 mM) and incubated in the dark for 30 min at 37 ℃. After incubation, the samples were centrifuged at 3500 rpm/min for 5 min, the supernatant were discharged, and the samples were washed twice with PBS. Finally, 400 µL PBS were added to resuspend the sperm pellet. The fluorescence was analyzed quantitatively by flow cytometry (Beckman-Coulter, France). Dead cells and detritus were excluded via a primary gate based on physical factors (forward and side light scatter). This experiment used 488 and 525 nm excitation and emission wavelengths.

Measurement of Intracellular Iron

We estimated the iron content in sperm using an iron ion colorimetric detection kit (Applygen, China). We collected sperm (20×10^6/mL) and lysed them with 200 µL RIPA buffer (Beyotime, China). The lysis was performed using ultrasonography on ice. A diluted standard stock solution was made immediately according to the manufacturer's instructions. Working reagents were prepared according to the manufacturer's instructions. First, the sample was incubated for an hour at 60 °C and then for 30 min at room temperature with 30 µL of iron ion detection reagent. The concentration of iron ions was measured at 550 nm with a microplate reader (Thermo Scientific, USA). Values are expressed as nmol of iron/10^8 sperm.

Measurement of Malondialdehyde (MDA)

MDA is produced during lipid peroxidation (LPO) and can react with thiobarbituric acid (TBA) to form a red-colored adduct, MDA-(TBA). Briefly, sperm were collected and homogenized in RIPA buffer (Beyotime, China). After centrifugation at $13{,}000 \times g$ for 10 min at room temperature, the supernatant was collected for quantitative analysis using an MDA assay kit (Nanjing Jiancheng Bioengineering Institute, China) according to the manufacturer's protocols. The absorbance was measured using a microplate reader (Thermo Scientific, USA) at a wavelength of 532 nm. Values are expressed as nmol of MDA/10^8 sperm.

Determination of Mitochondrial Membrane Potential

An MMP detection kit (JC-1) (Beyotime, China) was used according to the manufacturer's instructions. In summary, 20×10^6 sperm were resuspended in 0.5 mL BWW medium and combined with a 500 µL JC-1 working solution before being incubated at 37 °C for 30 min in the dark. After, samples were centrifuged for 5 min at $600 \times g$ (4 ℃), and the pellet was then washed twice with JC-1 buffer solutions and resuspended in 400 µL JC-1 buffer solution. The fluorescence was assessed in a flow cytometer (Beckman-Coulter, France) with excitation and emission settings of 488 nm and 525 nm (FL1 channel), respectively, and the percentage of stained cells was recorded as the population of sperm with a high $\Delta\Psi m$. The data are presented as the average percentage of high-$\Delta\Psi m \pm$ SEM.

Quantitative Real-Time PCR (qRT-PCR)

As recommended by the manufacturer, total RNA was extracted using RNAiso plus (Takara Bio, China). The PrimeScript™ RT reagent kit was used to reverse-transcribed whole RNA to cDNA (Takara Bio, China). Sequence-specific primers were used to express genes on a Bio-Rad CFX-96 cycler with SYBR Premix Ex Taq TM II (Takara Bio, China) (Bio-Rad Laboratories, USA). GAPDH was used to assess accuracy during the normalization process. All of the primer sequences found in Sangon of China are listed in Table 1 (Sangon).

Western Blot

RIPA (Beyotime, China) was used to extract proteins from spermatozoa on ice, and a BCA assay kit was used to assess the protein concentrations in the extracts (Beyotime, China). Using 10% sodium dodecyl sulfate–polyacrylamide gel electrophoresis, 40 µg of denatured protein was separated and transferred to a polyvinylidene difluoride membrane (Millipore, USA). After, for 2 h at room temperature, the PVDF membranes were blocked with 5% nonfat milk. Primary anti-GAPDH (1:5000; Millipore, USA), anti-SLC7A11 (1:3000, Boster, China), and anti-GPX4 (1:1000; Huabio, China) antibodies were then incubated with the membranes as directed by the manufacturer. Next, the membranes were incubated with horseradish peroxidase-conjugated goat anti-rabbit secondary antibody (1:5000; Boster, China) at room temperature for 1 h. The specific immunoreactive protein bands were developed with chemiluminescent HRP substrate reagent (Beyotime, China). GAPDH was used as an internal control for normalization.

Statistical Analysis

GraphPad Prism 8.0.2 was used for all analyses. Data were statistically described in terms of mean and standard deviation and percentages when appropriate. The Kolmogorov–Smirnov test was used to assess whether the distribution of variables was normal. To compare the means of continuous variables between asthenozoospermic and normozoospermic individuals, an independent *t* test or a Mann–Whitney test was employed. Correlations between variables were evaluated using Pearson's *r* correlation coefficient. $p < 0.05$ was considered statistically significant.

Table 1 Characteristics of the primers designed for target gens in the real-time PCR

Genes	Sequence (5′ – 3′)
SLC7A11	ATGCAGTGGCAGTGACCTTT GGCAACAAAGATCGGAACTG
GPX4	GCACATGGTTAACCTGGACA CTGCTTCCCGAACTGGTTAC
GAPDH	ACATCGCTCAGACACCATG TGTAGTTGAGGTCAATGAAGGG

Results

Clinical Parameters Between Asthenozoospermic and Normozoospermic Individuals

Sperm parameters between asthenozoospermia and normozoospermia are presented in Table 2. The normozoospermic individuals had considerably higher progressive motility, total motility, sperm viability, and sperm morphology than the asthenozoospermic individuals ($p < 0.01$) (Table 2). However, there was no difference between the two groups regarding age or ejaculate volume.

Iron and Oxidative Damage Were Accumulated in Asthenozoospermic Individuals

To explore the ferroptosis level between asthenozoospermic and normozoospermic individuals, ROS, MDA, and iron levels were detected in human sperm. Compared with the normozoospermic group, the content of ROS was significantly higher in the asthenozoospermic group ($p < 0.05$) (Fig. 1a), and an increase in MDA was also observed in asthenozoospermia ($p < 0.001$) (Fig. 1b), indicating that there was a high level of oxidative stress in the asthenozoospermic group. Meanwhile, the level of iron was also increased ($p < 0.001$) (Fig. 1c). Taken together, these data showed that there was a high ferroptosis level in the asthenozoospermic group.

The Mitochondrial Membrane Potential of the Asthenozoospermic Group Was Decreased

Usually, there is mitochondrial damage in ferroptosis [26]. The mitochondria with a low ΔΨm may be generators of free radicals in human spermatozoa that are dysfunctional [27, 28]. We found different changes in MMP (ΔΨm) between asthenozoospermia and normozoospermia. Representative results in the two groups are shown in Fig. 2a and b. Fluorescence microscopy was used to obtain images (Olympus, Japan). High membrane potential was detected in healthy mitochondria and generated red fluorescence, whereas green fluorescence was produced in mitochondria with a decreased membrane potential. The statistical results indicated that the MMP (ΔΨm) was decreased by 38.55% in asthenozoospermic individuals compared with normozoospermic individuals ($p < 0.05$) (Fig. 2c). Consistent with Fig. 2, there was an increased ratio of green to red fluorescence in asthenozoospermic sperm (Fig. 3).

Ferroptosis-Related Signaling Pathways Were Activated in Men with Asthenozoospermia

To explore the mechanism of ferroptosis in asthenozoospermic and normozoospermic patients, GPX4 and SLC7A11, two key regulators of the ferroptosis signaling pathway, were determined in human spermatozoa. Men with normozoospermia and infertile men with asthenozoospermia had mean *SLC7A11* mRNA expression levels of 1.683 ± 0.804 and 0.649 ± 0.302, respectively. Comparing the normozoospermic and asthenozoospermic groups, this parameter was greater in the former ($p < 0.001$) (Fig. 4a). Meanwhile, there was a significant difference in *GPX4* mRNA levels between sperm from asthenozoospermic and normozoospermic individuals ($p < 0.001$) (Fig. 4b). Furthermore, according to the western blot analysis, the protein expression of GPX4 and SLC7A11 was reduced in semen samples from asthenozoospermic patients relative to normozoospermic controls (Fig. 4c, d, and e). Correlation analysis between *GPX4* and *SLC7A11* and sperm clinical parameters and ferroptosis indicators were shown in Table 3 and Fig. 5. Based on our results, a significantly positive relationship was observed between *GPX4* expression and sperm progress motility and total motility ($r = 0.397$, $p = 0.009$; $r = 0.389$, $p = 0.011$) but not in iron, MDA, and MMP ($r = -0.276$, $p = 0.077$; $r = 0.199$, $p = 0.206$; $r = 0.201$, $p = 0.254$) (Fig. 5a, Table 3).

Table 2 Characteristics and semen analyses of the study population

Parameters	Group		*p*
	Normozoospermic ($n = 45$)	Asthenozoospermic ($n = 42$)	
Age (years)	30.38 ± 0.61	32.71 ± 0.96	0.393
Semen volume (ml)	3.62 ± 0.25	3.245 ± 0.22	0.258
Sperm concentration ($10^{\wedge 6}$/ml)	115.2 ± 10.72	76.94 ± 7.75	$< 0.01^{**}$
Total motility (%)	52.57 ± 1.25	20.67 ± 1.10	$< 0.001^{***}$
Sperm viability (%)	68.93 ± 0.98	34.07 ± 1.70	$< 0.001^{***}$
Progression motility (%)	47.54 ± 1.22	18.17 ± 1.63	$< 0.001^{***}$
Sperm morphology (%)	10.56 ± 0.55	5.96 ± 0.54	$< 0.001^{***}$

Data represent as mean ± SD

$^{**}p < 0.01$, $^{***}p < 0.001$

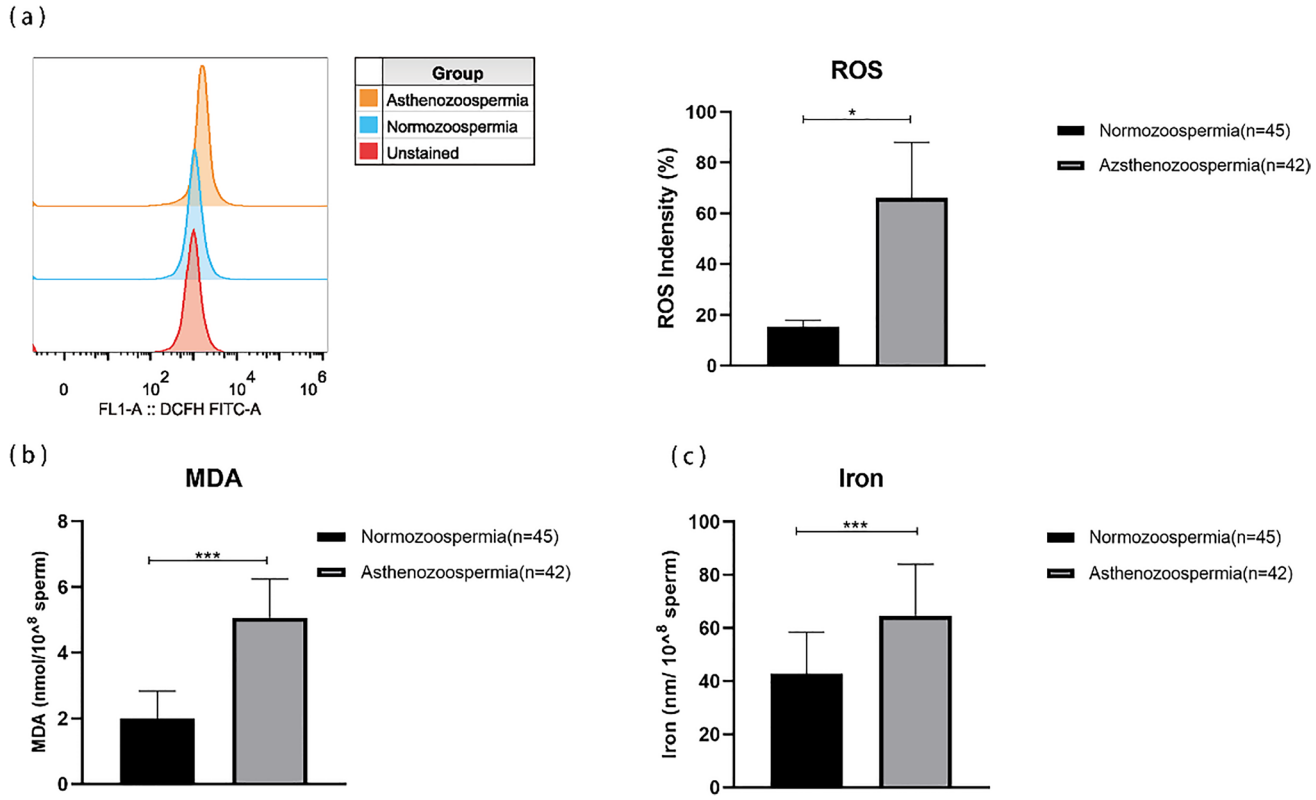

Fig. 1 ROS, MDA, and iron level in normozoospermic and asthenozoospermic individuals. **a** Representative data and statistical analysis and comparison of ROS in normozoospermic versus asthenozoospermic group. **b** Statistical analysis and comparison of MDA in normozoospermic versus asthenozoospermic group. **c** Statistical analysis and comparison of iron in normozoospermic versus asthenozoospermic group. *$p < 0.05$ and ***$p < 0.001$ represent the statistical difference compared to the respective group

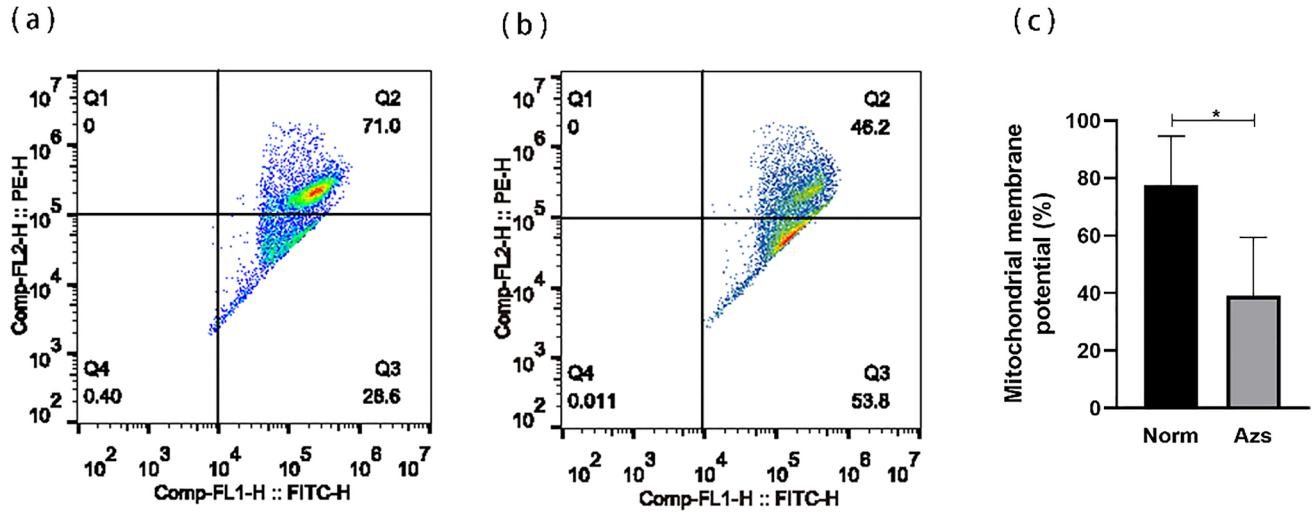

Fig. 2 Mitochondrial membrane potential (MMP) of spermatozoa in normozoospermic and men with asthenozoospermia. Representative data of MMP in normozoospermic (**a**) and asthenozoospermic individuals (**b**). JC-1 labels mitochondria with a high membrane potential red (JC-1 aggregates) and mitochondria with a low membrane potential green (JC-1 monomers). Sperm staining orange appears in the upper right quadrant (UR); green-stained spermatozoa appear in the lower right quadrant (LR). **c** Statistical analysis and comparison of MMP in normozoospermic versus asthenozoospermic group. *$p < 0.05$ represents the statistical difference compared to the respective group

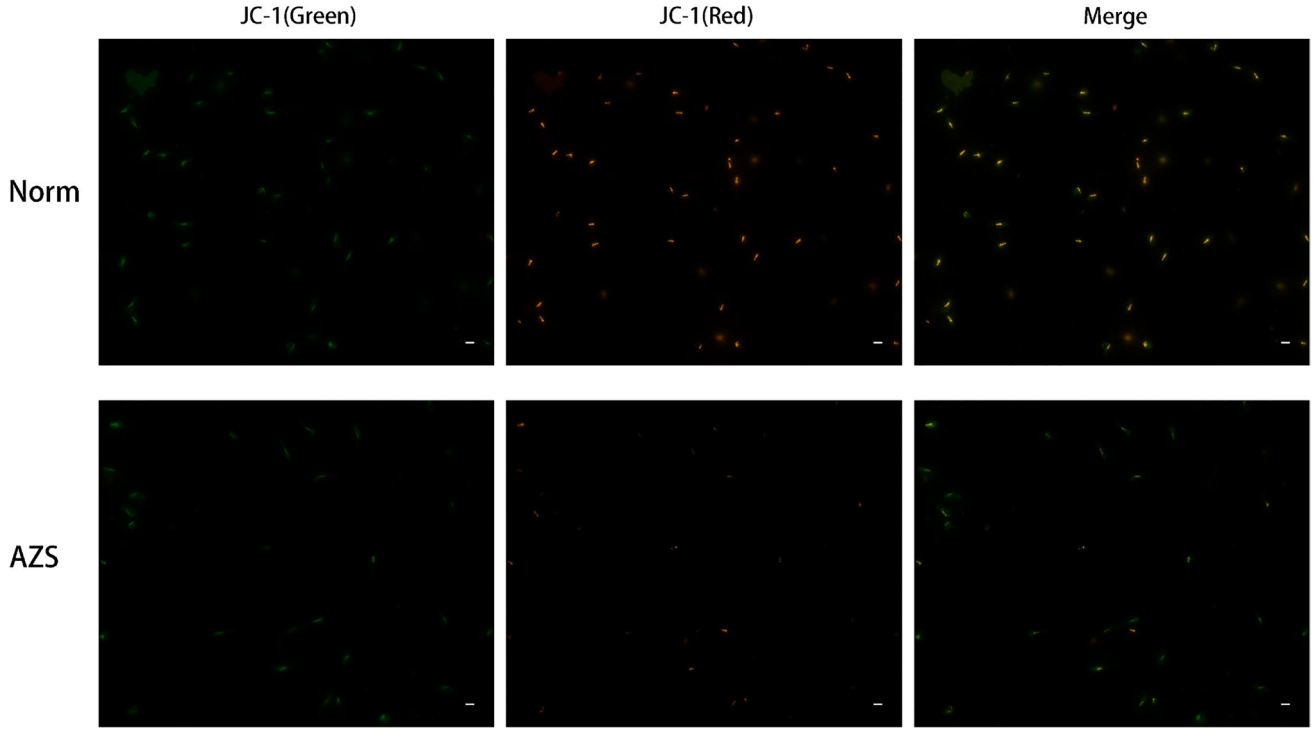

Fig. 3 Immunoassay photos of MMP in normozoospermic and men with asthenozoospermia. JC-1 was used to estimate the MMP of the spermatozoa, and the shift in the JC-1 fluorescence from red to green indicates a collapse of the MMP. The representative examples of one sperm are shown. The JC-1 aggregate image shows red fluorescence, and the JC-1 monomer image shows green fluorescence. In one sperm, both red fluorescence and green fluorescence can be seen under a fluorescent microscope. The merged image combines red and green images. Magnification × 400. Scale bar represents 25 μm

Alternatively, a possible positive correlation between sperm progress motility, total motility, and *SLC7A11* expression was observed($r = 0.275$, $p = 0.078$; $r = 0.267$, $p = 0.081$) (Fig. 5d, e). However, there were no significant correlations between iron, MDA, MMP, and *SLC7A11*($r = -0.079$, $p = 0.618$; $r = -0.253$, $p = 0.105$; $r = -0.081$, $p = 0.633$) (Fig. 5b, Table 3).

Discussion

This is the first study to explore the mechanism of ferroptosis in asthenozoospermia. Here, a case–control study was conducted between the asthenozoospermic group and normozoospermic group. Our results showed that asthenozoospermic men had higher levels of ROS, MDA, and iron, but MMP, SLC7A11, and GPX4 levels were lower. Therefore, we propose that the upregulated level of ferroptosis can reduce sperm motility by disturbing oxides and antioxidants in the spermatozoa of asthenozoospermic men (Fig. 6).

Oxidative stress has a critical role in asthenozoospermia [29, 30]. Polyunsaturated fatty acids (PUFAs) are abundant in spermatozoa and are highly reactive when exposed to free radicals. Polyunsaturated fatty acids are required to keep sperm membranes fluid and fusogenic, which is important for the acrosome reaction and sperm–egg interactions [31, 32]. Due to the unique architecture of human sperm, featuring an abundance of oxidizable substrates and limited intracellular antioxidant defenses, sperm is particularly vulnerable to elevated levels of ROS. In the present study, we found a high level of ROS in the sperm of the asthenozoospermic group, indicating that there is an imbalance between peroxidation and antioxidant scavenging in asthenozoospermic individuals. Consistent with our results, Vatannejad demonstrated that high levels of ROS can impair sperm motility by overwhelming antioxidant defense systems [8]. Other studies also revealed that asthenozoospermic men exhibit increased ROS, negatively affecting sperm function [29, 33].

As a type of regulated cell death, ferroptosis occurs when cells become overloaded with free iron due to an increase in radicals (ROS), lipid peroxidation, and membrane degradation. Several studies have shown that ferroptosis occurs in various human disorders [15, 34]. For example, several tumor cells are susceptible to ferroptosis inducers, indicating a new therapeutic strategy for cancer therapy [35–37]. In previous research, suppressing ferroptosis significantly reduced myocardial I/R damage, demonstrating that ferroptosis may play a vital role in the

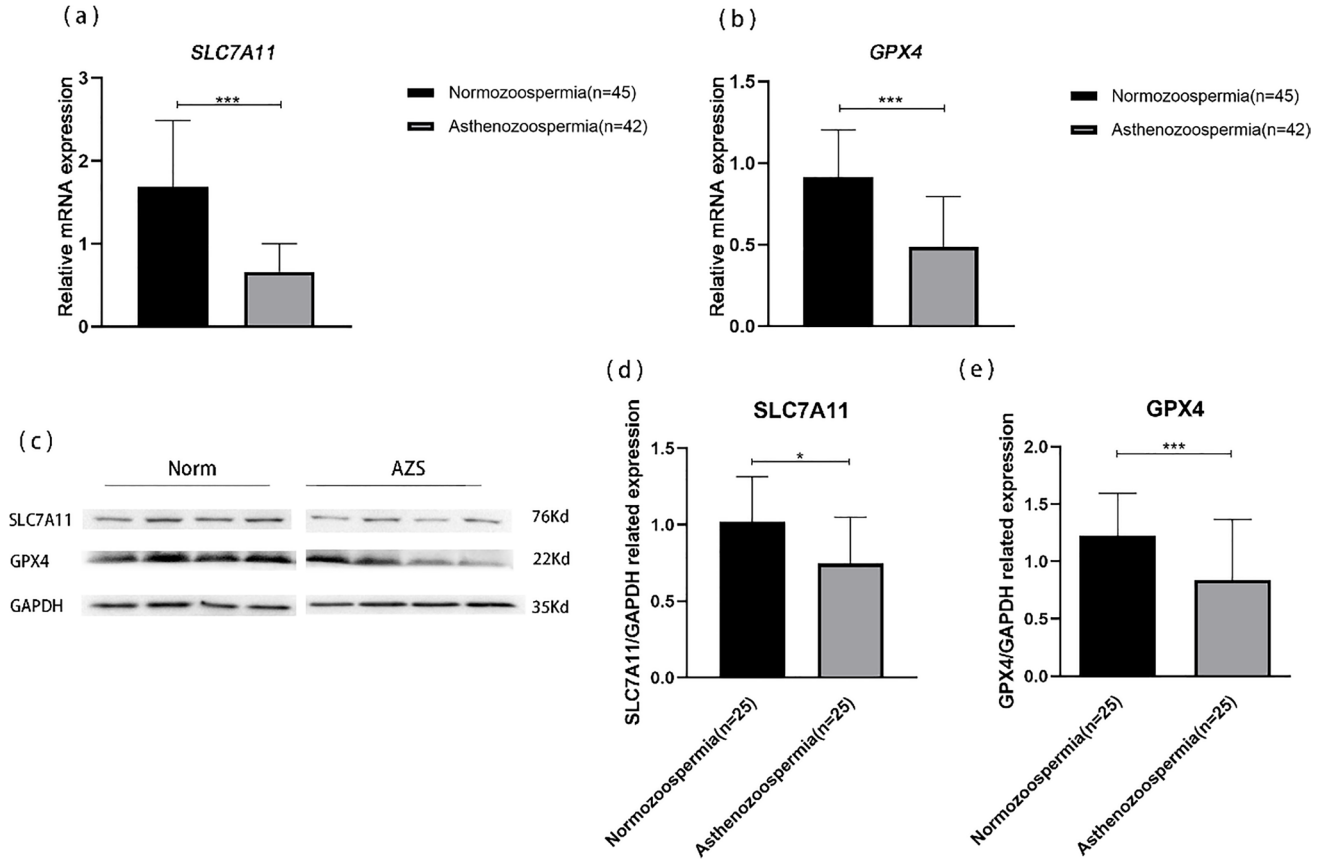

Fig. 4 Comparison of SLC7A11 and GPX4 expression between normozoospermic and asthenozoospermic individuals. Relative mRNA expression of *SLC7A11* (**a**) and *GPX4* (**b**) between the normozoospermic and asthenozoospermic groups. **c** Representative wb data of SLC7A11 and GPX4. Statistical analysis and comparison of SLC7A11 (**d**) and GPX4 (**e**) in normozoospermic versus asthenozoospermic group. $^{*}p<0.05$,$^{**}p<0.01$, and $^{***}p<0.001$ represent the statistical difference compared to the respective group

Table 3 Correlation between *GPX4*, *SLC7A11* mRNA expression, and clinical parameters and ferroptosis indicators in asthenozoospermia patients ($n=42$)

		Progressive motility	Total motility	Normal morphology	Viability	MDA	Iron	MMP
GPX4	*r*	0.397	0.389	0.102	0.012	0.199	−0.276	0.201
	p	0.009**	0.011*	0.520	0.307	0.206	0.077	0.254
SLC7A11	*r*	0.275	0.267	0.102	0.153	−0.253	−0.078	−0.086
	p	0.078	0.081	0.368	0.333	0.105	0.618	0.633

*$p<0.05$, **$p<0.01$

development of reperfusion injury and overall myocardial infarction (MI) [38]. Recently, direct in vivo study performed by Meng showed that the male reproductive toxicity of arsenite was manifested by ferroptosis [16]. In our study, we found that MDA, the indicator of lipid peroxidation, was significantly increased in the asthenozoospermia group. We next measured cellular iron, which acts as the main source of cellular ROS and lipid oxide formation through Fenton reaction and was also increased in asthenozoospermic sperm. Combining these findings, we determined that asthenozoospermic male sperm had a higher ferroptosis level.

Changes in mitochondrial pathology and function are distinctive features of ferroptosis [13, 39]. Mitochondria of human mature sperm play a key role in the maintenance of sperm motility by generating optimal levels of ROS and ATP [40, 41]. In mature sperm, mitochondria are essential to produce ATP, which provide sufficient energy for asymmetric flagellar beating and maintains sperm motility [42]. Moreover, interruption of mitochondrial electron transport

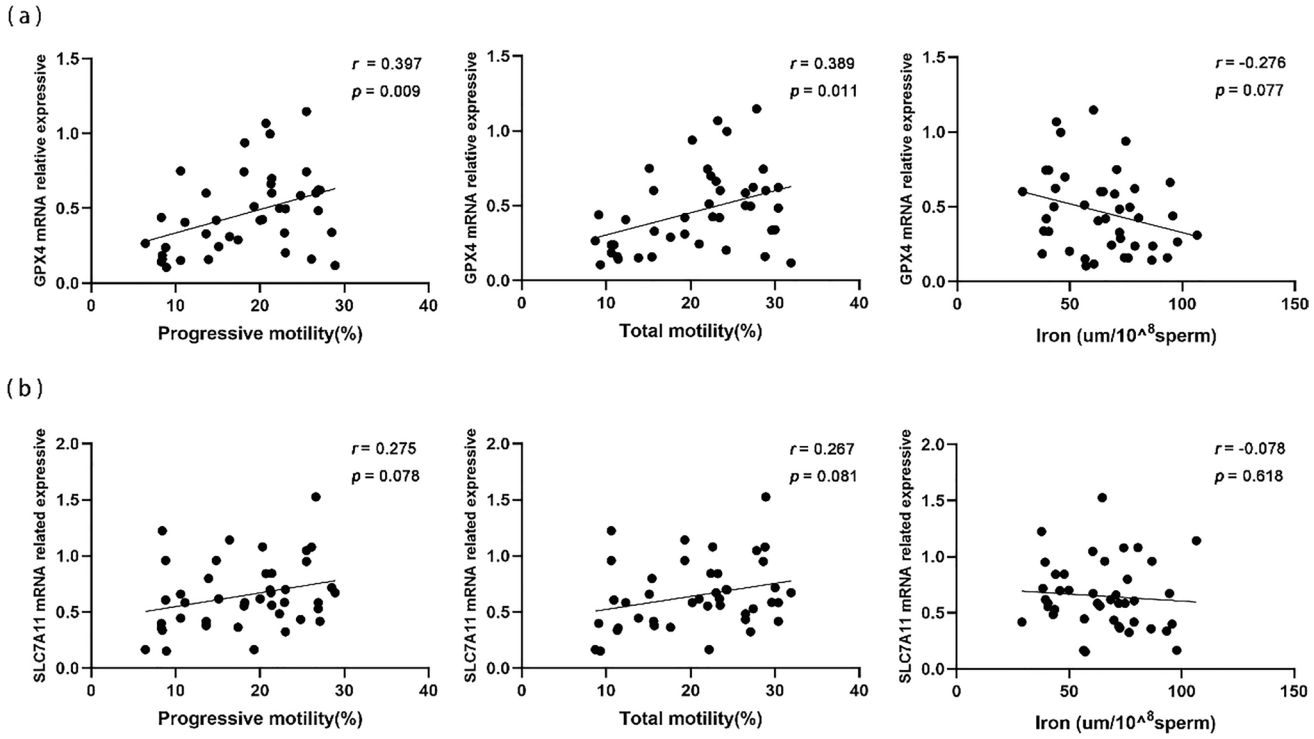

Fig. 5 Correlation analysis between *GPX4* and *SLC7A11* with sperm parameters. Correlations between sperm *GPX4* (**a**), *SLC7A11* (**b**), and percent of progressive motility, total motility, and iron in asthenozoospermia participants

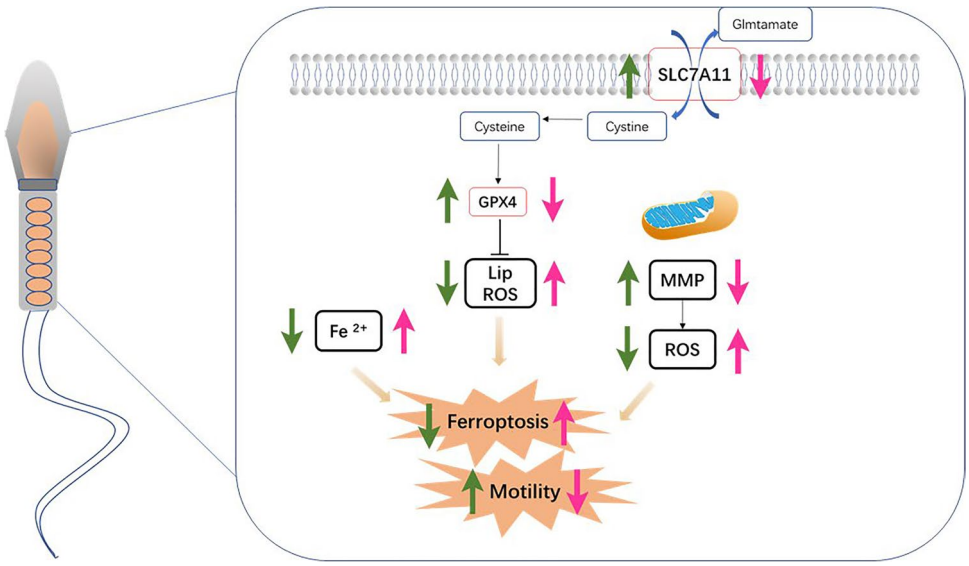

Fig. 6 Simplified model of the molecular mechanisms underlying the ferroptosis in sperm. Under physiological conditions (green arrow), SLC7A11 and GPX4, together with Fe^{2+} and MMP, protect sperm from ferroptosis. Once SLC7A11 is downregulated (pink arrow), the subsequent depletion of GPX4 and Fe^{2+}-oxidized lipids generates a large amount of lip ROS, while the reduced MMP also results in the accumulation of ROS, both of which promote ferroptosis and finally result in a loss of motility in human spermatozoa. SLC7A11, solute carrier family 7 members 11; GPX4, GSH-dependent peroxidase 4; MMP, mitochondrial membrane potential; ROS, reactive oxygen species

flow resulted in the production of reactive oxygen species (ROS) on the matrix side of the inner mitochondrial membrane in complex I (MCI), resulting in peroxidative damage and a loss of motility in human spermatozoa [43, 44]. To confirm a decreased MMP level as previously reported, JC-1 was used to examine mitochondrial dysfunction. The results indicated that the MMP ($\Delta\Psi m$) was decreased in the asthenozoospermic group, consistent with the previous study. Based on these findings, we propose that ferroptosis levels are increased in the sperm of asthenozoospermic men and that abnormalities in ferroptosis levels lead to dysfunction of the mitochondrial electron transport chain, ultimately resulting in a MMP decline.

To further analyze mechanisms underlying the occurrence of ferroptosis in asthenozoospermia, changes in GPX4 and SLC7A11 were observed. GPX4 is the key molecule of keeping ferroptosis in check and acts as an antioxidant defense enzyme in cells, whereas conditions that culminate in GPX4 inhibition can trigger ferroptosis cell death [45, 46]. As part of system Xc^-, SLC7A11 serves as a key transporter of amino acids, moving cystine from the extracellular space and reducing it to cysteine to help with glutathione (GSH) synthesis. Additionally, reducing the expression of SLC7A11 is linked to a lower activity of GPX4 [47]. Currently, most scholars agree that the primary cellular defense pathway against ferroptosis is the SLC7A11-GPX4 signaling axis [48–50]. Interestingly, evidence has shown that the GPX4 content of human sperm was positively correlated with sperm count, motility, and structural integrity, and the activity of GPX4 in mature human spermatozoa was associated with fertility-related parameters [51]. Consistent with previous reports, significantly reduced expression of GPX4 and positive correlations between *GPX4* and progressive motility and total motility were found in asthenozoospermia group in the present study. However, the asthenozoospermic group had lower levels of SLC7A11 than the control group. We also observed a possible correlation between SLC7A11 expression and sperm motility, although the data was not significant. These data suggested that GPX4 and SLC7A11 may play vital roles in maintaining sperm motility.

According to previous studies, GPX4 is a part of the mitochondria of human sperm [51, 52], so we speculated that the reduction in GPX4 in sperm may affect mitochondrial function. However, in the present study, we found no significant correlation between *GPX4* mRNA expression and sperm MMP. GPX4 has three different isoforms derived from the same gene, the cytosolic (cGPX4), mitochondrial (mGPX4), and sperm nuclear (snGPX4) forms [53, 54], so it is likely to speculate that mGPX4, but not other GPX4 isoform, may be closely related to mitochondrial function. Meanwhile, because glutamate is important for the tricarboxylic acid (TCA) cycle anaplerosis and mitochondrial respiration [55, 56], we proposed that SLC7A11, an export of glutamate [57], may have a role in maintaining mitochondrial function. However, we did not observe a significant correlation between SLC7A11 and MMP in our data. We hypothesized that the difference here could be because oxidative phosphorylation (OXPHOS) is the major energy system for sperm but not the TCA cycle [58]. These findings imply that by suppressing SLC7A11 expression and depleting GPX4, GSH metabolism is disrupted, lipid peroxide cannot be catalyzed and reduced by GPX4, and Fe^{2+}-oxidized lipids produce a large amount of reactive oxygen species (ROS) via the Fenton reaction, all of which promote ferroptosis and contribute to sperm motility reduction in asthenozoospermic males. However, the mechanism of ferroptosis and the associated signaling pathway responsible for regulating cell death still need further research.

In conclusion, this study demonstrates that in asthenozoospermia patients, the reduction of MMP, GPX4, and SLC7A11, together with the increased lipid ROS and iron, led to ferroptosis in sperm and resulted a decrease in sperm motility. Inhibiting ferroptosis, a novel therapeutic target for asthenozoospermia, may have a role in treating male infertility.

Author Contribution All authors contributed to the study conception and design. JPM designed this study; XLH and HW performed the experiments and statistical analysis and drafted the manuscript; LY and RH collected the semen samples; FC and ZHY collected the data.

Data Availability Will be provided on request.

Declarations

Ethics Approval and Consent to Participate Ethics approval was obtained from the First Affiliated Hospital of Chongqing Medical University's Ethics Committee (2021–266) for all study techniques.

Consent to Participate The written informed consent was obtained from all the subjects enrolled in this study.

Consent for Publication Not applicable.

Conflict of Interest The authors declare no competing interests.

References

1. Jiang Q, Maresch CC, Petry SF, Paradowska-Dogan A, Bhushan S, Chang Y, et al. Elevated CCL2 causes Leydig cell malfunction in metabolic syndrome. JCI Insight. 2020;5(21):e134882.
2. Hwang K, Walters RC, Lipshultz LI. Contemporary concepts in the evaluation and management of male infertility. Nat Rev Urol. 2011;8(2):86–94.
3. Shen Y, Zhang F, Li F, Jiang X, Yang Y, Li X, et al. Loss-of-function mutations in QRICH2 cause male infertility with multiple morphological abnormalities of the sperm flagella. Nat Commun. 2019;10(1):433.
4. Nowicka-Bauer K, Lepczynski A, Ozgo M, Kamieniczna M, Fraczek M, Stanski L, et al. Sperm mitochondrial dysfunction

and oxidative stress as possible reasons for isolated asthenozoospermia. J Physiol Pharmacol. 2018;69(3):403–17.
5. Whitfield M, Thomas L, Bequignon E, Schmitt A, Stouvenel L, Montantin G, et al. Mutations in DNAH17, encoding a sperm-specific axonemal outer dynein arm heavy chain, cause isolated male infertility due to asthenozoospermia. Am J Hum Genet. 2019;105(1):198–212.
6. Sironen A, Shoemark A, Patel M, Loebinger MR, Mitchison HM. Sperm defects in primary ciliary dyskinesia and related causes of male infertility. Cell Mol Life Sci. 2020;77(11):2029–48.
7. Liu H, Guo W, Guo H, Zhao L, Yue L, Li X, et al. Bakuchiol attenuates oxidative stress and neuron damage by regulating Trx1/TXNIP and the phosphorylation of AMPK after subarachnoid hemorrhage in mice. Front Pharmacol. 2020;11:712.
8. Vatannejad A, Tavilani H, Sadeghi MR, Karimi M, Lakpour N, Amanpour S, et al. Evaluation of the NOX5 protein expression and oxidative stress in sperm from asthenozoospermic men compared to normozoospermic men. J Endocrinol Invest. 2019;42(10):1181–9.
9. Barati E, Nikzad H, Karimian M. Oxidative stress and male infertility: current knowledge of pathophysiology and role of antioxidant therapy in disease management. Cell Mol Life Sci. 2020;77(1):93–113.
10. Vatannejad A, Tavilani H, Sadeghi MR, Amanpour S, Shapourizadeh S, Doosti M. Evaluation of ROS-TAC score and DNA damage in fertile normozoospermic and infertile asthenozoospermic males. Urol J. 2017;14(1):2973–8.
11. Huang XK, Huang YH, Huang JH, Liang JY. Glutathione S-transferase P1 Ile105Val polymorphism and male infertility risk: an updated meta-analysis. Chin Med J. 2017;130(8):979–85.
12 Ghafarizadeh AA, Vaezi G, Shariatzadeh MA, Malekirad AA. Effect of in vitro selenium supplementation on sperm quality in asthenoteratozoospermic men. Andrologia. 2018;50(2):e12869.
13. Dixon SJ, Lemberg KM, Lamprecht MR, Skouta R, Zaitsev EM, Gleason CE, et al. Ferroptosis: an iron-dependent form of nonapoptotic cell death. Cell. 2012;149(5):1060–72.
14. Li Y, Zeng X, Lu D, Yin M, Shan M, Gao Y. Erastin induces ferroptosis via ferroportin-mediated iron accumulation in endometriosis. Hum Reprod. 2021;36(4):951–64.
15. Ajoolabady A, Aslkhodapasandhokmabad H, Libby P, Tuomilehto J, Lip GYH, Penninger JM, et al. Ferritinophagy and ferroptosis in the management of metabolic diseases. Trends Endocrinol Metab. 2021;32(7):444–62.
16. Meng P, Zhang S, Jiang X, Cheng S, Zhang J, Cao X, et al. Arsenite induces testicular oxidative stress in vivo and in vitro leading to ferroptosis. Ecotoxicol Environ Saf. 2020;194: 110360.
17. Ou Z, Wen Q, Deng Y, Yu Y, Chen Z, Sun L. Cigarette smoking is associated with high level of ferroptosis in seminal plasma and affects semen quality. Reprod Biol Endocrinol. 2020;18(1):55.
18. Zhao X, Liu Z, Gao J, Li H, Wang X, Li Y, et al. Inhibition of ferroptosis attenuates busulfan-induced oligospermia in mice. Toxicology. 2020;440: 152489.
19. Krabbendam IE, Honrath B, Dilberger B, Iannetti EF, Branicky RS, Meyer T, et al. SK channel-mediated metabolic escape to glycolysis inhibits ferroptosis and supports stress resistance in C. elegans. Cell Death Dis. 2020;11(4):263.
20. Yang WS, SriRamaratnam R, Welsch ME, Shimada K, Skouta R, Viswanathan VS, et al. Regulation of ferroptotic cancer cell death by GPX4. Cell. 2014;156(1–2):317–31.
21. Nakamura BN, Lawson G, Chan JY, Banuelos J, Cortés MM, Hoang YD, et al. Knockout of the transcription factor NRF2 disrupts spermatogenesis in an age-dependent manner. Free Radical Biol Med. 2010;49(9):1368–79.
22. Sun L, Dong H, Zhang W, Wang N, Ni N, Bai X, et al. Lipid peroxidation, GSH depletion, and SLC7A11 inhibition are common causes of EMT and ferroptosis in A549 cells, but different in specific mechanisms. DNA Cell Biol. 2021;40(2):172–83.
23 Uchida D, Takaki A, Adachi T, Okada H. Beneficial and paradoxical roles of anti-oxidative nutritional support for non-alcoholic fatty liver disease. Nutrients. 2018;10(8):977.
24. Liu T, Jiang L, Tavana O, Gu W. The deubiquitylase OTUB1 mediates ferroptosis via stabilization of SLC7A11. Can Res. 2019;79(8):1913–24.
25. Zhang HT, Luo H, Wu J, Lan LB, Fan DH, Zhu KD, et al. Galangin induces apoptosis of hepatocellular carcinoma cells via the mitochondrial pathway. World J Gastroenterol. 2010;16(27):3377–84.
26. Tian Y, Lu J, Hao X, Li H, Zhang G, Liu X, et al. FTH1 inhibits ferroptosis through ferritinophagy in the 6-OHDA model of Parkinson's disease. Neurotherapeutics. 2020;17(4):1796–812.
27. Barbonetti A, Vassallo MR, Di Rosa A, Leombruni Y, Felzani G, Gandini L, et al. Involvement of mitochondrial dysfunction in the adverse effect exerted by seminal plasma from men with spinal cord injury on sperm motility. Andrology. 2013;1(3):456–63.
28. Barbonetti A, Castellini C, Di Giammarco N, Santilli G, Francavilla S, Francavilla F. In vitro exposure of human spermatozoa to bisphenol A induces pro-oxidative/apoptotic mitochondrial dysfunction. Reprod Toxicol. 2016;66:61–7.
29. Moazamian R, Polhemus A, Connaughton H, Fraser B, Whiting S, Gharagozloo P, et al. Oxidative stress and human spermatozoa: diagnostic and functional significance of aldehydes generated as a result of lipid peroxidation. Mol Hum Reprod. 2015;21(6):502–15.
30. Maghsoumi-Norouzabad L, Zare Javid A, Mansoori A, Dadfar M, Serajian A. Evaluation of the effect of vitamin D supplementation on spermatogram, seminal and serum levels of oxidative stress indices in asthenospermia infertile men: a study protocol for a triple-blind, randomized controlled trial. Nutr J. 2021;20(1):49.
31. Alahmar AT. Role of oxidative stress in male infertility: an updated review. J Hum Reprod Sci. 2019;12(1):4–18.
32. Sapanidou VG, Margaritis I, Siahos N, Arsenopoulos K, Dragatidou E, Taitzoglou IA, et al. Antioxidant effect of a polyphenol-rich grape pomace extract on motility, viability and lipid peroxidation of thawed bovine spermatozoa. J Biol Res (Thessalonike). 2014;21(1):19.
33 Opuwari CS, Henkel RR, Muratori M. An update on oxidative damage to spermatozoa and oocytes. BioMed Res Int. 2016;2016:1–11.
34. Otasevic V, Vucetic M, Grigorov I, Martinovic V, Stancic A. Ferroptosis in different pathological contexts seen through the eyes of mitochondria. Oxid Med Cell Longev. 2021;2021:5537330.
35. Sun X, Ou Z, Chen R, Niu X, Chen D, Kang R, et al. Activation of the p62-Keap1-NRF2 pathway protects against ferroptosis in hepatocellular carcinoma cells. Hepatology (Baltimore, MD). 2016;63(1):173–84.
36. Roh JL, Kim EH, Jang H, Shin D. Nrf2 inhibition reverses the resistance of cisplatin-resistant head and neck cancer cells to artesunate-induced ferroptosis. Redox Biol. 2017;11:254–62.
37. Hong T, Lei G, Chen X, Li H, Zhang X, Wu N, et al. PARP inhibition promotes ferroptosis via repressing SLC7A11 and synergizes with ferroptosis inducers in BRCA-proficient ovarian cancer. Redox Biol. 2021;42: 101928.
38. Tang LJ, Luo XJ, Tu H, Chen H, Xiong XM, Li NS, et al. Ferroptosis occurs in phase of reperfusion but not ischemia in rat heart following ischemia or ischemia/reperfusion. Naunyn-Schmiedeberg's Arch Pharmacol. 2021;394(2):401–10.
39. Doll S, Freitas FP, Shah R, Aldrovandi M, da Silva MC, Ingold I, et al. FSP1 is a glutathione-independent ferroptosis suppressor. Nature. 2019;575(7784):693–8.
40. Koppers AJ, De Iuliis GN, Finnie JM, McLaughlin EA, Aitken RJ. Significance of mitochondrial reactive oxygen species in the

generation of oxidative stress in spermatozoa. J Clin Endocrinol Metab. 2008;93(8):3199–207.
41. Chai R-R, Chen G-W, Shi H-J, Wai-Sum O, Martin-DeLeon PA, Chen H. Prohibitin involvement in the generation of mitochondrial superoxide at complex I in human sperm. J Cell Mol Med. 2017;21(1):121–9.
42. Morita M, Suwa R, Iguchi A, Nakamura M, Shimada K, Sakai K, et al. Ocean acidification reduces sperm flagellar motility in broadcast spawning reef invertebrates. Zygote (Cambridge, England). 2010;18(2):103–7.
43. Marchetti C, Obert G, Deffosez A, Formstecher P, Marchetti P. Study of mitochondrial membrane potential, reactive oxygen species, DNA fragmentation and cell viability by flow cytometry in human sperm. Hum Reprod. 2002;17(5):1257–65.
44 Umezu K, Kurata S, Takamori H, Numabe T, Hiradate Y, Hara K, et al. Characteristics and possible role of bovine sperm head-to-head agglutination. Cells. 2020;9(8):1865.
45. Seibt TM, Proneth B, Conrad M. Role of GPX4 in ferroptosis and its pharmacological implication. Free Radical Biol Med. 2019;133:144–52.
46. Wang X, Xu S, Zhang L, Cheng X, Yu H, Bao J, et al. Vitamin C induces ferroptosis in anaplastic thyroid cancer cells by ferritinophagy activation. Biochem Biophys Res Commun. 2021;551:46–53.
47. Lin CH, Lin PP, Lin CY, Lin CH, Huang CH, Huang YJ, et al. Decreased mRNA expression for the two subunits of system xc(-), SLC3A2 and SLC7A11, in WBC in patients with schizophrenia: evidence in support of the hypo-glutamatergic hypothesis of schizophrenia. J Psychiatr Res. 2016;72:58–63.
48. Koppula P, Zhuang L, Gan B. Cystine transporter SLC7A11/xCT in cancer: ferroptosis, nutrient dependency, and cancer therapy. Protein Cell. 2021;12(8):599–620.
49. Koppula P, Zhang Y, Zhuang L, Gan B. Amino acid transporter SLC7A11/xCT at the crossroads of regulating redox homeostasis and nutrient dependency of cancer. Cancer Commun (Lond). 2018;38(1):12.
50. Friedmann Angeli JP, Schneider M, Proneth B, Tyurina YY, Tyurin VA, Hammond VJ, et al. Inactivation of the ferroptosis regulator Gpx4 triggers acute renal failure in mice. Nat Cell Biol. 2014;16(12):1180–91.
51. Imai H, Suzuki K, Ishizaka K, Ichinose S, Oshima H, Okayasu I, et al. Failure of the expression of phospholipid hydroperoxide glutathione peroxidase in the spermatozoa of human infertile males. Biol Reprod. 2001;64(2):674–83.
52. Foresta C, Flohé L, Garolla A, Roveri A, Ursini F, Maiorino M. Male fertility is linked to the selenoprotein phospholipid hydroperoxide glutathione peroxidase. Biol Reprod. 2002;67(3):967–71.
53. Brigelius-Flohé R, Flohé L. Regulatory phenomena in the glutathione peroxidase superfamily. Antioxid Redox Signal. 2020;33(7):498–516.
54. Wanagat J, Dai D-F, Rabinovitch P. Mitochondrial oxidative stress and mammalian healthspan. Mech Ageing Dev. 2010;131(7–8):527–35.
55. Zhu J, Schwörer S, Berisa M, Kyung YJ, Ryu KW, Yi J, et al. Mitochondrial NADP(H) generation is essential for proline biosynthesis. Science. 2021;372(6545):968–72.
56. Robinson MB, Lee ML, DaSilva S. Glutamate transporters and mitochondria: signaling, co-compartmentalization, functional coupling, and future directions. Neurochem Res. 2020;45(3):526–40.
57. Koppula P, Zhang Y, Shi J, Li W, Gan B. The glutamate/cystine antiporter SLC7A11/xCT enhances cancer cell dependency on glucose by exporting glutamate. J Biol Chem. 2017;292(34):14240–9.
58 Park Y-J, Pang M-G. Mitochondrial functionality in male fertility: from spermatogenesis to fertilization. Antioxidants (Basel, Switzerland). 2021;10(1):98.